CSMA 2026
17ème Colloque National en Calcul des Structures
18-22 Mai 2026, Presqu'île de Giens (Var)

An extended finite element method for sloshing problems involving immersed structures at arbitrary positions

H. Bouvet[1], A. Legay[1], L. Laurent[1], C. Hoareau[1]

[1] *LMSSC, Conservatoire National des Arts et Métiers, 292 Rue Saint-Martin, Paris 75003, France, hippolyte.bouvet@lecnam.net.*

Abstract — When subjected to dynamic excitations, liquid-filled tanks are particularly prone to sloshing, a phenomenon that can become critical in rockets, tank trucks or liquid storage facility, where it may lead to a loss of control or ultimate damage. A common mitigation strategy is to introduce internal baffles in order to attenuate fluid motion. A numerical method is developed to address a general sloshing problem while accounting for the discontinuity in the pressure field induced by an internal tank baffle modeled as a shell. The approach relies on a partition of unity strategy (XFEM), which eliminates the need for remeshing and rebuilding of operators for each baffle position and shape. This feature enables an efficient geometric parametrization and greatly facilitates subsequent optimization procedures.The proposed method is implemented for a three-dimensional fluid and validated on a parallelepiped tank sloshing problem with an internal baffle under harmonic excitation.
Keywords — fluide-structure interaction, sloshing, XFEM.

1 Introduction

Liquid-filled tanks are encountered in many engineering fields. When subjected to dynamic excitations, they are particularly prone to sloshing phenomena. This effect can become critical in rockets, tank trucks or liquid storage facility, where it may lead to a loss of control and/or critical damages on structure. Historically, the first systematic investigations of sloshing dynamics were conducted in the 1950s by NASA [1], motivated by the need to derive mechanically equivalent models of liquid motion to support feedback-control strategies for spacecraft and launch vehicles. With the rapid development of computational resources in subsequent decades, sloshing problems have increasingly been addressed using finite volume techniques [2]. More recently, studies [3] have shown that isogeometric analysis (IGA) can be particularly effective for solving sloshing problems, especially in tanks with complex geometries. In parallel, several works demonstrated that the introduction of internal baffles can be particularly effective in mitigating fluid motion [4]. Beyond these aspects, the modelling challenge further increases when fluid–structure interaction must be considered, especially due to the potentially nonlinear structural response of a thin structure undergoing large displacements, together with the potentially nonlinear behaviour of the fluid. Nevertheless, in industrial design offices, the primary challenge remains the reduction of computational cost, especially when repeated evaluations are required for parametric studies or optimization loops, involving the tank geometry itself or the shape and position of the internal baffle. In this context, the approach of this present work relies on a partition of unity strategy (XFEM) [5], which eliminates the need for remeshing and the repeated reconstruction of the associated operators for each baffle position and shape. This feature enables an efficient geometric parametrization and is intended to greatly facilitate subsequent optimization procedures in future developments. It is also worth noting that sloshing problems are traditionally addressed in the time domain; in contrast, the present work formulates the problem in the frequency domain which avoids the costly time integration, and directly provides key engineering quantities such as FRFs and harmonic pressure fields. This makes it particularly well suited for design and optimization contexts, where computational efficiency is critical.

In the following, we first introduce the governing equations and the XFEM-based discretization of a generic sloshing problem. The proposed method is then implemented for a three-dimensional fluid in a parallelepiped tank with an internal baffle under harmonic excitation. The parametrization of the baffle

geometry is detailed, together with the numerical procedure enabling the computations of the pressure fields and efficient frequency-response computations.

2 Strong and weak forms of a sloshing problem

2.1 Description of the problem

A fluid–structure interaction problem is considered and illustrated in Figure 1. The fluid domain and the thin flexible structure are respectively denoted by Ω_F and Ω_S. The problem is studied in the frequency domain for a permanent harmonic response at angular frequency ω. The fluid domain is described using pressure p and displacement $\boldsymbol{u}_F$, whereas displacement $\boldsymbol{u}_S$ is used for the structural part. Their boundaries are separated into

— imposed Dirichlet boundary condition on the structure denoted $\partial_1\Omega_S$,
— prescribed Neumann boundary condition on the structure denoted $\partial_2\Omega_S$,
— coupling interface between the fluid and the structural domain, excluding the baffle region, denoted Σ,
— coupling interface between fluid and the baffle denoted $\partial\Omega_S^F$, and
— the free surface of the fluid domain Γ.

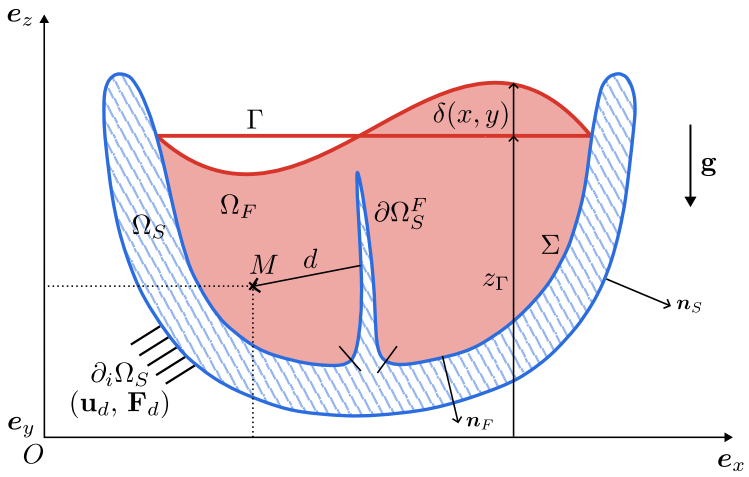

FIGURE 1 – Description and notations for a generic sloshing problem with an immersed baffle.

We denote $\partial\Omega_S = \partial_1\Omega_S \cup \partial_2\Omega_S \cup \Sigma \cup \partial\Omega_S^F$ the boundary of the structural domain and $\partial\Omega_F = \Gamma \cup \Sigma \cup \partial\Omega_S^F$ the boundary of the fluid domain.

2.2 Strong form of the equations

2.2.1 Structure

The structural domain is assumed satisfying the elastodynamic linearized equation at angular frequency ω, within the framework of the small-perturbation assumption :

$$\mathbf{div}(\boldsymbol{\sigma}_S) + \omega^2 \rho_S \, \boldsymbol{u}_S = \mathbf{0} \qquad \text{in } \Omega_S, \tag{1}$$

where ρ_S is the constant density per unit volume and $\boldsymbol{\sigma}_S$ is the Cauchy stress tensor, given by

$$\boldsymbol{\sigma}_S = \boldsymbol{D}_S : \boldsymbol{\varepsilon}(\boldsymbol{u}_S) \qquad \text{in } \Omega_S, \tag{2}$$

where $\boldsymbol{D}_S$ is the classical Hooke's linear elasticity tensor and $\boldsymbol{\varepsilon}(\boldsymbol{u}_S)$ is the strain tensor associated to the displacement vector field $\boldsymbol{u}_S$, defined by

$$\boldsymbol{\varepsilon}(\boldsymbol{u}_S) = \frac{1}{2}(\mathbf{grad}\ \boldsymbol{u}_S + \mathbf{grad}^T \boldsymbol{u}_S) \tag{3}$$

Prescribed harmonic displacements and forces are imposed on the external structural boundaries $\partial_1\Omega_S$ and $\partial_2\Omega_S$, respectively, in order to simulate the dynamic loading that may be experienced by a tank.

$$\boldsymbol{u}_S = \boldsymbol{u}_\mathrm{d} \qquad \text{on } \partial_1\Omega_S, \tag{4}$$

$$\boldsymbol{\sigma}_S \cdot \boldsymbol{n}_S = \boldsymbol{F}_\mathrm{d} \qquad \text{on } \partial_2\Omega_S, \tag{5}$$

where $\boldsymbol{n}_S$ is the unit normal vector pointing outward from the structure domain.

2.2.2 Fluid

The liquid is considered to behave as an idealized continuum satisfying several simplifying assumptions. The analysis is carried out by decomposing the total pressure field p_t into a static p_s and a dynamic contribution p, allowing the separation of the hydrostatic equilibrium from the unsteady effects induced by the sloshing motion, such as

$$p_t(M,\omega) = p_s(M) + p(M,\omega), \tag{6}$$

where $p_s(M) = p_0 + \rho_F g(z_\Gamma - z)$, with p_0 denoting the atmospheric pressure and z_Γ the elevation of the undisturbed free surface as illustrated in Figure 1.

The fluid is assumed to be perfect (or inviscid), meaning that viscous effects are neglected. Consequently, no vorticity is generated during the motion, and since the liquid is initially at rest, the flow remains irrotational throughout the motion. The liquid density is assumed to be constant and homogeneous, which leads to the incompressibility condition. In this framework, the motion of an inviscid and incompressible fluid is governed by the Euler equations. For small-amplitude oscillations, the nonlinear convective term is negligible, allowing the use of the linearized form. The equations resulting from these assumptions can be written in the frequency domain as

$$\boldsymbol{\sigma}_F = -p_t \boldsymbol{I} \qquad \text{in } \Omega_F, \tag{7}$$

$$-\omega^2 \rho_F \boldsymbol{u}_F = -\mathbf{grad}\ p_t + \rho_F \boldsymbol{g} \qquad \text{in } \Omega_F, \tag{8}$$

where ρ_F is the fluid density and $\boldsymbol{g} = -g\boldsymbol{e}_z$ the gravitational acceleration vector (Figure 1).

Taking the divergence of Equation (8) with Equation (6) and using the incompressibility condition yields

$$\Delta p = 0 \qquad \text{in } \Omega_F, \tag{9}$$

which shows that the dynamic pressure field p satisfies Laplace's equation within the fluid domain. By combining Equations (6) and (8), the following condition is obtained on the boundary of the fluid domain :

$$\mathbf{grad}\ p \cdot \boldsymbol{n}_F = \omega^2 \rho_F \boldsymbol{u}_F \cdot \boldsymbol{n}_F \qquad \text{on } \partial\Omega_F, \tag{10}$$

where $\boldsymbol{n}_F$ is the unit normal vector pointing outward from the fluid domain. On the free surface Γ, the linearized dynamic and kinematic conditions can be combined to yield the following boundary relation :

$$\mathbf{grad}\ p \cdot \boldsymbol{n}_F = \frac{\omega^2}{g} p \qquad \text{on } \Gamma. \tag{11}$$

The elevation above the undisturbed free surface, as illustrated in Figure 1 is given by [6] :

$$\delta(x,y) = \frac{p(x,y,z_\Gamma)}{\rho_F g} \tag{12}$$

2.2.3 Fluid–structure coupling

At interface between the structural domain and the fluid, normal stress and normal displacement continuity conditions are given by

$$\boldsymbol{\sigma}_S \cdot \boldsymbol{n}_S - p\,\boldsymbol{n}_F = 0 \qquad \text{on } \Sigma \cup \partial\Omega_S^F, \tag{13}$$

$$(\boldsymbol{u}_F - \boldsymbol{u}_S) \cdot \boldsymbol{n}_F = 0 \qquad \text{on } \Sigma \cup \partial\Omega_S^F. \tag{14}$$

2.3 Weak form

The test-function method is used to derive the variational formulation of the coupled problem. For this purpose, the spaces of sufficiently smooth functions $C_{\boldsymbol{u}_s}$ and C_p are introduced, associated to the field variables $\boldsymbol{u}_s$ and p, respectively.

Let $\boldsymbol{v}$ be the frequency-independent test function, associated to $\boldsymbol{u}_s$, belonging to the admissible space $C^*_{\boldsymbol{u}_s} = \{\boldsymbol{v} \in C_{\boldsymbol{u}_s} \mid \boldsymbol{v} = 0 \quad \text{on } \partial_1\Omega_S\}$. Multiplying Equation (1) combined with (2) by $\boldsymbol{v} \in C^*_{\boldsymbol{u}_s}$, applying a Green's formula, and taking Equation (13) into account leads to

$$\int_{\Omega_s} \boldsymbol{\sigma} : \varepsilon(\boldsymbol{v}) \mathrm{dV} - \omega^2 \int_{\Omega_S} \rho_S \boldsymbol{u}_s \cdot \boldsymbol{v} \mathrm{dV} - \int_{\partial\Omega_S^F} p\boldsymbol{v} \cdot \boldsymbol{n}_F \mathrm{dS} = 0. \tag{15}$$

Let q be the frequency-independent test function, associated to p, belonging to the admissible space C_p. Multiplying Equation (9) by $q \in C_p$, applying a Green's formula, and taking Equations (4), (11) and (14) into account leads to

$$\int_{\Omega_F} \mathbf{grad}\; p \cdot \mathbf{grad}\; q \;\mathrm{dV} - \frac{\omega^2}{g} \int_{\Gamma} qp \mathrm{dS} \; - \omega^2 \int_{\partial\Omega_S^F} \rho_F q \boldsymbol{u}_S \cdot \boldsymbol{n}_F \mathrm{dS} = \omega^2 \int_{\Sigma} \rho_F q \boldsymbol{u}_d \cdot \boldsymbol{n}_F \mathrm{dS} \tag{16}$$

3 Discontinuous discretization of the fluid using XFEM

The baffle induces a pressure discontinuity across its interface. This discontinuity can be handled using a conforming mesh, where the nodes along the baffle are duplicated, thereby introducing additional degrees of freedom. However, in the context of a parametric study involving variations in the baffle position and shape, such an approach requires remeshing and rebuilding the operators for each set of design parameters, which can become computationally expensive. In this work, to correctly catch the pressure jump from one side of the structure to the other one, the pressure field approximation is enriched by a Heaviside function using a partition of unity strategy [7], namely XFEM [5].

The thin structure is considered with no thickness in the fluid domain meaning that the structure is seen by the fluid as surfaces. These surfaces are described in the fluid domain by the zero contour of a level-set $\phi(M)$ that is the signed distance to the closest structure. By denoting d the distance of a point M to the structure as illustrated in Figure 1, the level-set can be defined as

$$\phi(M) = \pm d, \tag{17}$$

where d is the minimal distance to the structure ; the sign is determined using a conventional unit normal vector $\boldsymbol{n}$ pointing arbitrarily outward of one side of the baffle.

The pressure approximation becomes :

$$p(M) = \sum_{i \in \mathcal{F}} N_F^i(M) P_i + \sum_{i \in \mathcal{A}} N_F^i(M) \psi_i(M) A_i \tag{18}$$

where $\mathcal{F}$ is the set of the $n_{\mathcal{F}}$ nodes of the whole mesh, $N_F^i(M)$ is the shape function associated to the fluid node i, P_i is the standard nodal pressure value, $\mathcal{A}$ is the set of the $n_{\mathcal{A}}$ enriched nodes, $\psi_i(M)$ is the enrichment function [8], and A_i is the additional nodal unknown coming from the enrichment. A node is

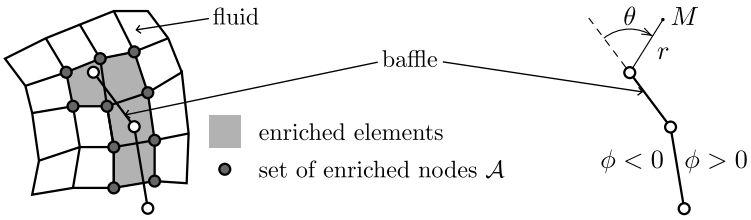

FIGURE 2 – XFEM mesh and angular coordinate θ used for enrichment function treatment at the tip of the baffle.

classified as enriched when it lies within an element intersected by the structural interface, corresponding to the zero level-set contour as shown on Figure 2. The total number of degrees of freedom in the system is thus $n_{\mathcal{F}} + n_{\mathcal{A}}$, implying that only a small number of additional degrees of freedom $n_{\mathcal{A}}$ is introduced relative to the size of the fluid mesh. The associated enrichment function along the baffle is defined such that

$$\psi(M) = H(\phi(M)), \tag{19}$$

where H is the Heaviside function and $\phi(M)$ is the signed distance function. The Heaviside function is modified to be the sign of the level-set. At the tip of the baffle, immersed within the fluid, an additional treatment is required to properly account for the discontinuity of the enrichment function, which undergoes a jump from $+1$ to -1. This singularity can be addressed by enforcing continuity of the enrichment function for the points located above the tip [8], with the angular coordinate θ being used to distinguish whether a point lies above or below this geometric feature as shown in Figure 2.

Finally, the enrichment function ψ is expressed as

$$\psi(M) = \begin{cases} H(\phi(M)) & \text{if } |\theta| > \dfrac{\pi}{2}, \\ \dfrac{2}{\pi}\theta & \text{if } |\theta| < \dfrac{\pi}{2}. \end{cases} \tag{20}$$

The full approximation containing both the standard part and the enrichment can be written from Equation (18) as

$$p(M) = \boldsymbol{N}_F(M)\,\mathbf{P} + \boldsymbol{N}_A(M)\,\boldsymbol{A}, \tag{21}$$

where

$$\boldsymbol{N}_A(M) = \psi(M)\boldsymbol{N}_F(M)\boldsymbol{\beta}_{FA}. \tag{22}$$

The Boolean localization matrix $\boldsymbol{\beta}_{FA}$ is used to extract enriched set of nodes $\mathcal{A}$ from the set of nodes $\mathcal{F}$. The pressure value at an enriched node $i \in \mathcal{A}$ is then

$$p(M_i) = P_i + \psi(M_i)A_i. \tag{23}$$

4 Discretization of the coupled problem

4.1 Discretized weak form

By replacing the continuous pressure field as well as the structure displacements by their approximations in Equations (15) and (16), the following discretized system is obtained :

$$\left(\begin{bmatrix} \mathbf{H}_{\mathrm{FF}} & \mathbf{H}_{\mathrm{FA}} & \mathbf{0} \\ \mathbf{H}_{\mathrm{FA}}^T & \mathbf{H}_{\mathrm{AA}} & \mathbf{0} \\ \mathbf{0} & -\mathbf{C}_{\mathrm{SA}} & \mathbf{K}_{\mathrm{SS}} \end{bmatrix} - \omega^2 \begin{bmatrix} \mathbf{S}_{\mathrm{FF}} & \mathbf{S}_{\mathrm{FA}} & \mathbf{0} \\ \mathbf{S}_{\mathrm{FA}}^T & \mathbf{S}_{\mathrm{AA}} & \mathbf{C}_{\mathrm{SA}}^T \\ \mathbf{0} & \mathbf{0} & \mathbf{M}_{\mathrm{SS}} \end{bmatrix} \right) \begin{bmatrix} \mathbf{P} \\ \mathbf{A} \\ \mathbf{U}_{\mathrm{S}} \end{bmatrix} = \begin{bmatrix} \mathbf{C}_{\mathrm{F}} \\ \mathbf{0} \\ \mathbf{F}_{\mathrm{S}} \end{bmatrix}, \tag{24}$$

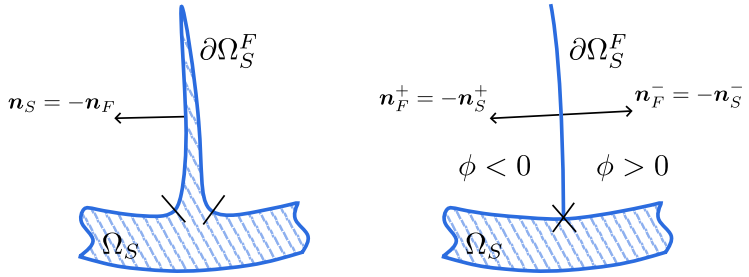

FIGURE 3 – Interface coupling details.

where $\mathbf{K}_{\mathrm{SS}}$ and $\mathbf{M}_{\mathrm{SS}}$ are respectively the stiffness and mass matrices of the structure, $\mathbf{F}_{\mathrm{S}}$ is the discretized external load on the structure and $\mathbf{C}_{\mathrm{F}}$ is the contribution from the imposed acceleration on the structure, expressed as

$$\mathbf{C}_{\mathrm{F}} = \int_{\partial_1\Omega_S} -\omega^2 \rho_F \, \boldsymbol{N}_{\mathrm{F}}^T \, \boldsymbol{n}_F^T \, \boldsymbol{u}_d \, \mathrm{dS}, \tag{25}$$

where $\boldsymbol{N}_{\mathrm{F}}$ is the matrix of shape functions associated to the fluid nodes and $\ddot{\boldsymbol{u}}_d$ is the imposed acceleration on the structure.

The other matrices are defined as :

$$\mathbf{H}_{\mathrm{FF}} = \int_{\Omega_F} \boldsymbol{B}_{\mathrm{F}}^T \boldsymbol{B}_{\mathrm{F}} \, \mathrm{dV}, \qquad \mathbf{S}_{\mathrm{FF}} = \int_{\Gamma} \boldsymbol{N}_{\mathrm{F}}^T \boldsymbol{N}_{\mathrm{F}} \, \mathrm{dS}, \tag{26}$$

$$\mathbf{H}_{\mathrm{FA}} = \int_{\Omega_F} \boldsymbol{B}_{\mathrm{F}}^T \boldsymbol{B}_{\mathrm{A}} \, \mathrm{dV}, \qquad \mathbf{S}_{\mathrm{FA}} = \int_{\Gamma} \boldsymbol{N}_{\mathrm{F}}^T \boldsymbol{N}_{\mathrm{A}} \, \mathrm{dS}, \tag{27}$$

$$\mathbf{H}_{\mathrm{AA}} = \int_{\Omega_F} \boldsymbol{B}_{\mathrm{A}}^T \boldsymbol{B}_{\mathrm{A}} \, \mathrm{dV}, \qquad \mathbf{S}_{AA} = \int_{\Gamma} \boldsymbol{N}_{\mathrm{A}}^T \boldsymbol{N}_{\mathrm{A}} \, \mathrm{dS}, \tag{28}$$

$$\mathbf{C}_{\mathrm{AS}} = 2 \int_{\partial\Omega_S^F} \boldsymbol{N}_{\mathrm{A}}^T \boldsymbol{n}_F^{+T} \boldsymbol{N}_{\mathrm{S}} \, \mathrm{dS}, \tag{29}$$

where $\boldsymbol{B}_{\mathrm{F}}$ is the discretized gradient matrix of the shape functions associated with the fluid nodes, $\boldsymbol{N}_{\mathrm{S}}$ is the matrix of shape functions associated to the structure nodes, $\boldsymbol{n}_F^+$ is the normal vector defined on Figure 3 whose orientation is assigned according to the sign of ϕ and $\boldsymbol{B}_{\mathrm{A}}$ is expressed from Equation (22) such that :

$$\boldsymbol{B}_{\mathrm{A}} = \mathbf{grad}(\boldsymbol{N}_{\mathrm{A}}) = \psi(M) \, \boldsymbol{B}_{\mathrm{F}} \boldsymbol{\beta}_{\mathrm{FA}} + \mathbf{grad}(\psi(M)) \, \boldsymbol{N}_F(M) \boldsymbol{\beta}_{\mathrm{FA}}. \tag{30}$$

5 Results

A parallelepiped tank of length b and width a is considered in Figure 4, where h denotes the fluid height. A baffle is immersed in the fluid with a height $e < h$. The baffle is defined by four points : two points are fixed at the abscissa $x = d$, while the other two are parameterized by x_{down} and x_{up}, corresponding to the lower and upper points B and C, respectively, such that $x_B = d + x_{\mathrm{down}}$ and $x_C = d + x_{\mathrm{up}}$ ($x_{\mathrm{down}} < 0$ on Figure 4). An acceleration $\ddot{\boldsymbol{u}}_d = \ddot{\boldsymbol{u}}_0$ with $|\ddot{\boldsymbol{u}}_0| = \omega^2 u_0$ is imposed on the wall of the tank and the baffle within the $(O, \boldsymbol{e}_x, \boldsymbol{e}_y)$ plane, simulating the dynamic excitations that a tank may experience.

In the present study, the internal baffle, as well as the external tank walls, are assumed to be rigid and the internal baffle is modeled as a shell. Using Equation (10), the discretized formulation thus simplifies to

$$\left(\begin{bmatrix} \mathbf{H}_{\mathrm{FF}} & \mathbf{H}_{\mathrm{FA}} \\ \mathbf{H}_{\mathrm{FA}}^T & \mathbf{H}_{\mathrm{AA}} \end{bmatrix} - \omega^2 \begin{bmatrix} \mathbf{S}_{\mathrm{FF}} & \mathbf{S}_{\mathrm{FA}} \\ \mathbf{S}_{\mathrm{FA}}^T & \mathbf{S}_{\mathrm{AA}} \end{bmatrix} \right) \begin{bmatrix} \mathbf{P} \\ \mathbf{A} \end{bmatrix} = \begin{bmatrix} \omega^2 \rho_F \mathbf{U}_0 \\ \mathbf{0} \end{bmatrix}. \tag{31}$$

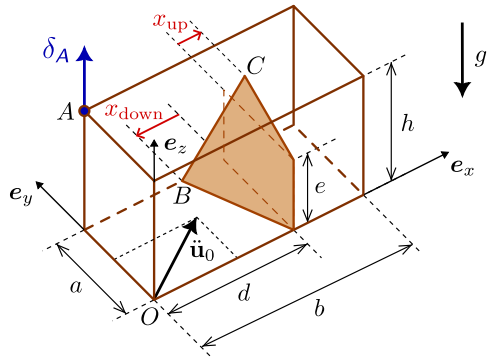

a	0.8 m
b	1 m
h	0.6 m
d	0.53 m
e	0.52 m

FIGURE 4 – Parallelepipedic tank with an immersed and parametrically defined baffle.

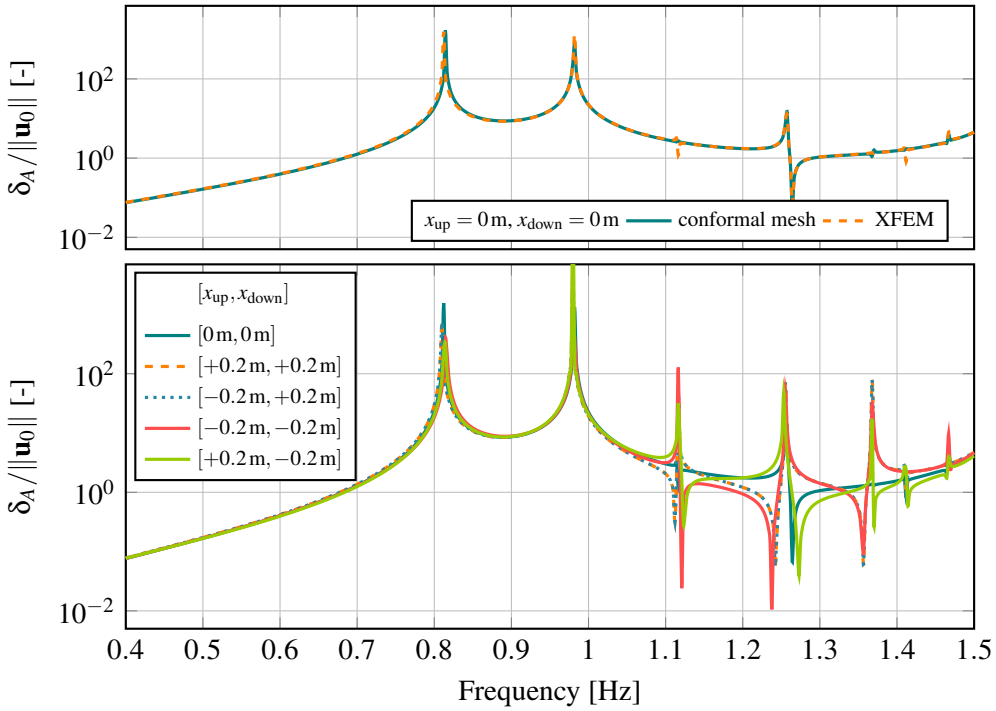

FIGURE 5 – Frequency response function (FRF) relative to the elevation at point A for different geometrical configurations of the baffle.

The objective of the study is to compute the frequency response of the cavity for various sets of parameters, and consequently for different geometrical configurations of the baffle. Solving Equation (31) enables the computation of the pressure field within the tank for various baffle geometries and excitation frequencies. On the Figure 5, the frequency response of the free-surface elevation at point A is computed from the pressure field on the undisturbed free surface using Equation (12). The comparison with a conformal mesh (the baffle's thickness is fixed to 2 mm) shows very good agreement of the XFEM approach. On the Figure 6, the pressure field is displayed for a selected baffle configuration, $x_{\text{up}} = 0.2\,\text{m}$, $x_{\text{down}} = -0.2\,\text{m}$ and for two distinct excitation frequencies.

The parameters significantly affect the frequency response, particularly above 1 Hz. It should be noted that no damping has been introduced in the fluid; therefore, infinite peaks are observed at the resonance frequencies. A fluctuation of the pressure field is observed, and the discontinuity introduced by the internal baffle, accounted for through the XFEM approach, is clearly visible. A consistent correlation is found between the elevation of point A at the resonance frequencies and the corresponding modal deformation of the pressure field.

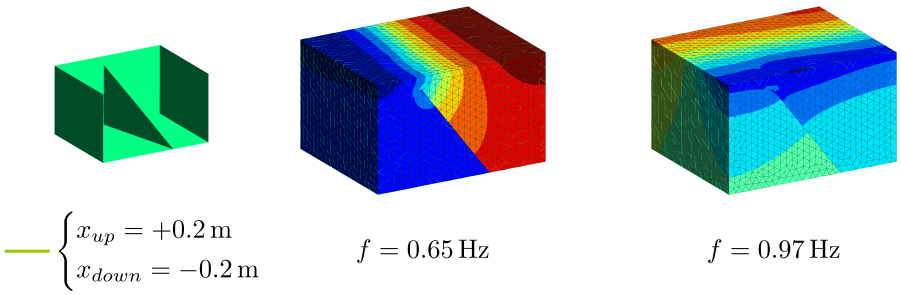

FIGURE 6 – Dynamic pressure field for a selected baffle configuration ($x_{\mathrm{up}} = +0.2\,\mathrm{m}$, $x_{\mathrm{down}} = -0.2\,\mathrm{m}$) and two distinct excitation frequencies.

6 Conclusion

A numerical strategy based on the eXtended Finite Element Method (XFEM) has been proposed to model sloshing phenomena in tanks containing rigid baffles. The governing equations were established in the frequency domain, and the pressure field is enriched by a Heaviside function to capture the discontinuity induced by the immersed structure. The discretized coupled system is implemented and applied to a three-dimensional tank under harmonic excitation, where both the external walls and the internal baffle were assumed to be rigid. The method successfully captures the discontinuity of the pressure field induced by the immersed structure while avoiding the computational cost of remeshing and rebuilding operators for each geometric configuration of baffle. The results show that the geometrical parameters strongly influence the frequency response, especially beyond 1 Hz.

This work forms the first step toward an extended framework, whose objective is to enable constrained, potentially multi-objective optimization involving numerous design parameters. Ultimately, the goal is to enhance the overall numerical efficiency of the solver–optimizer framework.

References

[1] H. N. ABRAMSON. *The dynamic behavior of liquids in moving containers, with applications to space vehicle technology*. Rapp. tech. National Aeronautics et Space Administration, 1966.

[2] M. JÄGER. *Fuel tank sloshing simulation using the finite volume method*. Springer, 2019.

[3] C. HOAREAU, J.-F. DEÜ et R. OHAYON. « Projection-based reduced order model and hyper-reduction of linear sloshing with geometric parameters using isogeometric analysis ». In : *Advanced Modeling and Simulation in Engineering Sciences* 12.1 (2025), p. 1-32.

[4] D. LIU et P. LIN. « Three-dimensional liquid sloshing in a tank with baffles ». In : *Ocean engineering* 36.2 (2009), p. 202-212.

[5] N. MOËS, J. DOLBOW et T. BELYTSCHKO. « A finite element method for crack growth without remeshing ». In : *International journal for numerical methods in engineering* 46.1 (1999), p. 131-150.

[6] F. T. DODGE. *The new "Dynamic Behavior of Liquids in Moving Containers"*. Update and revision of NASA SP-106 (1966). San Antonio, TX : Southwest Research Institute, 2000, p. 195.

[7] J. M. MELENK et I. BABUŠKA. « The partition of unity finite element method : basic theory and applications ». In : *Computer methods in applied mechanics and engineering* 139.1-4 (1996), p. 289-314.

[8] A. LEGAY. « The Extended Finite Element Method Combined with a Modal Synthesis Approach for Vibro-Acoustic Problems ». In : *International Journal for Numerical Methods in Engineering* 101.5 (2015), p. 329-350.